dc transport in dissipative disordered one-dimensional systems

R. Hey*
Institut für Physikalische Chemie, Johannes-Gutenberg-Universität, D-55099 Mainz, Federal Republic of Germany

K. Maschke
Institut de Physique Appliquée, Ecole Polytechnique Fédérale, CH-1015 Lausanne, Switzerland

M. Schreiber
Institut für Physik, Technische Universität Chemnitz-Zwickau, D-09107 Chemnitz, Federal Republic of Germany
(Received 13 February 1995)

We present a numerical study of the dc transport properties of dissipative disordered chains which are described by linear ensembles of interconnected scatterers. The elastic-scattering amplitudes are derived from an Anderson Hamiltonian with diagonal (site) disorder. Inelastic scattering is accounted for by connecting the sites of the Anderson chain to separate external electron reservoirs. The calculated wave-vector-dependent transmission probabilities are discussed for chains with different lengths and for different degrees of dissipation. Using the Landauer-Büttiker approach we obtain the dc resistance of the considered samples. Our results demonstrate the rather intricate competition between elastic and inelastic scattering.

I. INTRODUCTION

Electronic transport in mesoscopic samples is dominated by quantum interference effects.[1] A transparent description of the underlying physics is given by the approach of Landauer,[2] who relates the conductance of a quantum wire to its scattering properties at the Fermi energy. Such a quantum wire can be described by a chain of single scatterers, where each scatterer represents a lattice site of the chain. Mathematically, such single scatterers can be represented by the respective scattering matrices. The scattering matrix of the whole chain can then be calculated from the scattering matrices of the single scatterers. In this way, it is possible to take into account the multiple reflections between the single scatterers, which lead to quantum interference effects.

This model was used by Büttiker,[3] who introduced dissipative scattering in a phenomenological way by connecting the lattice sites of the chain to respective local external electron reservoirs via additional scattering channels. The coupling to these reservoirs is controlled by a parameter. Assuming that electrons scattered into the reservoirs will be thermalized before being reemitted into the chain, and imposing current conservation within the chain, it follows that each electron entering the reservoir is replaced by another electron which is injected from the reservoir back into the chain. The assumed thermalization in the reservoirs implies that the phases of the electrons reinjected from the reservoirs into the chain are not correlated with those of the entering electrons. Furthermore, their energies are determined by the statistical (equilibrium) energy distribution in the local reservoirs. Consequently, the coupling of the chain to the reservoirs provides a possibility to characterize the strength of inelastic scattering for the electron through the system. This approach enabled Büttiker to discuss the transport properties of linear chains consisting of elastic and inelastic scatterers.

Following these ideas, this model was recently extended to the case of generalized scatterers,[4] which allow for elastic as well as inelastic scattering according to paramatrized scattering probabilities. With this approach, transport properties of ordered systems have been extensively studied.[4,5] Disorder has also been introduced into these investigations by randomly varying the intersite separation (spatial disorder).[6,7] This is the most straightforward way to destroy the constructive or (possibly) destructive interference between the coherently multiply scattered waves. It was shown in the regime of destructive interference, i.e., small transmission probability, that the conductance can be enhanced by the introduction of spatial disorder, whereas in the regime of high transmission probability the conductance of disordered samples is always smaller than in the ordered system. This result can be translated into band-structure terminology: introduction of disorder leads to localized states in these band tails. We will show in this paper that this effect can also be achieved by introduction of inelastic scattering into an energetically disordered system: the conductance of a system with site-energy disorder can be enhanced or suppressed by inelastic scattering, depending on the choice of the electron wave vector q. A similar observation has recently been reported[7] for the spatially disordered chain.

D'Amato and Pastawski[8] have presented an extension of the Landauer approach, which enabled them to calculate the conductance of ordered and Anderson-disordered chains in the presence of inelastic scattering by means of a Green's function method. In their approach, the chain and the perfect leads, which couple the chain to the reservoirs, are characterized by a nearest-neighbor tight-binding Hamiltonian H. In this picture, the tight-binding

parameters in the lateral perfect wires control the coupling between chain and reservoirs. As pointed out by Datta,[9] such reservoirs can be represented by an ensemble of continuously distributed independent harmonic oscillators.

Recently, the Landauer approach has also been used to study the resistance of finite repeated structures[10] and the conductance of random dimer chains.[11] Random dimer models can be used to describe the structure of polymer chains such as polyaniline. Therefore it should be possible to describe elastic and inelastic electron transport in polymers within the Landauer-Büttiker approach using a nearest-neighbor tight-binding Hamiltonian and extend recent studies,[12,13] a subject on which we will focus in a forthcoming paper.

In the present paper we apply the Landauer-Büttiker theory to a disordered linear chain and present numerical studies on the transmission probabilities, resistance, and respective decay lengths of this system. In contrast to the above-mentioned spatial disorder, we introduce disorder by randomly choosing the site energies in the Hamiltonian from a uniform distribution (site disorder). Restricting ourselves for simplicity to nearest-neighbor transfer matrix elements, the elastic-scattering part of this model corresponds to the well-known Anderson model of localization.[14] The reflection and transmission coefficients at each lattice site can be derived in an elementary way[15] for this tight-binding linear chain. Following Ref. 4 we build up a scattering matrix for each lattice site including the inelastic scattering by means of a parametrized scattering strength. In this approach, the derivation of the elastic-scattering coefficients from the Anderson Hamiltonian avoids the necessity of a second phenomenological parameter.

From the single scattering matrices we calculate the total scattering matrix of the chain using an iterative algorithm.[6] The local chemical potential for the electron reservoir at each lattice site is determined from the current conservation conditions. The resistance can then be evaluated in terms of the chemical potentials and the transmission probabilities between the channels, which are obtained from the total scattering matrix.

II. THE MODEL

We consider a supramolecular system as a linear chain of sites. (The generalization to topologically more complex systems has been discussed elsewhere.[16]) The sites of the chain could be single atoms but could also comprise complicated molecules of, e.g., a polymer chain. The atomic and intramolecular vibrations as well as possible interactions with the surroundings (e.g., a solvent) constitute the heat bath at each site. Between the sites, the electrons are allowed to travel as freely moving particles, i.e., they are described by plane waves. Scattering of these waves takes place at the sites. In order to apply the scattering matrix technique to such a system, in which the electrons are also allowed to interact with the local environment, we consider a general scatterer, which comprises elastic as well as inelastic scattering. Such a scatterer is symbolically depicted in Fig. 1.

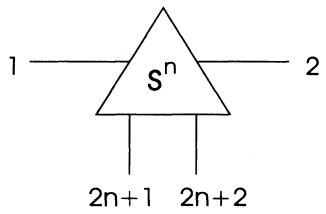

FIG. 1. Channels of a single scatterer at position n. Coupling with the heat bath takes place via the channels $2n+1$ and $2n+2$. Channels 1 and 2 are the transport channels.

Coherent transport takes place via the transport channels 1 and 2, governed by the reflection and transmission coefficients r and t of the single scatterers. Depending on the phases of incoming and outgoing waves, multiple elastic scattering at the sites can lead to either constructive or destructive interference of the plane waves. In addition, inelastic-scattering processes occur. If the electron is scattered inelastically at some lattice site n, it enters the electron reservoir via the side channels. Current conservation requires reinjection of the electron into the transport channel, but, as incoming and outgoing waves are not related to each other, this corresponds to an irreversible phase-breaking process.

Mathematically, we can describe such a scatterer by its scattering matrix

$$s^1=\begin{bmatrix} \alpha r & \alpha t & 0 & \beta \\ \alpha t & \alpha r & \beta & 0 \\ 0 & \beta & -\alpha r^* & -\alpha t^* \\ \beta & 0 & -\alpha t^* & -\alpha r^* \end{bmatrix}=(s_{ij}^1)\ , \tag{1}$$

with $i,j=1,2,3,4$ for the first scatterer ($n=1$) and $i,j=1,2,2n+1,2n+2$ for the general case in Fig. 1. The parameters α and β determine the relative strength of elastic and inelastic scattering:

$$\alpha=\sqrt{1-\varepsilon}\ , \tag{2}$$

$$\beta=\sqrt{\varepsilon}\ . \tag{3}$$

In the limit of $\varepsilon=0$, one obtains a completely elastic scatterer with no contribution of the side channels to the electron transport. On the other hand, if $\varepsilon=1$, transport occurs only via the side channels, leading to completely incoherent behavior.

We note that the zero matrix elements s_{13} and s_{24} depend on our particular choice of connecting the transport channels and the heat bath channels. A generalization is possible[17] but of no relevance in the present context. The choice of the matrix elements s_{ij} for $i,j=3,4$, on the other hand, is not arbitrary, but is determined by the requirement that the scattering matrix has to be unitary.

In principle, the scattering matrix elements s_{11} and s_{22} could differ by a phase, but this would mean an asymmetric scatterer, which can of course be introduced in a parametrized way. It cannot, however, be derived from a microscopic model for a (symmetric) point scatterer.

Such a microscopic description is our intention in the following.

To determine the reflection and transmission coefficients in the elastic part of the scattering matrix, we consider a plane wave with wave vector q (in units of π/a, where a is the nearest-neighbor spacing between the sites), which constitutes the Bloch wave that solves a simple tight-binding model with identical site energies E_0 and constant nearest-neighbor interaction V. (In the following we have chosen $V\equiv 1$ to define the energy scale and $E_0\equiv 0$ to fix the origin of the energy axis.) Introducing a single impurity into such an ordered system leads to elastic scattering. The respective reflection and transmission coefficients are given[15] by

$$r=\frac{-F}{F+2iV\sin(qa)}\ , \tag{4}$$

$$t=1+r\ , \tag{5}$$

where F is the deviation of the corresponding site energy from E_0. This can be generalized to a chain consisting only of such impurities. Then Eqs. (4) and (5) describe the elastic scattering at each site, depending on the respective site energy $F(n)$ which we choose randomly from a uniform distribution of width W in correspondence with the Anderson model of localization:[14] $F(n)\in[-W/2,W/2]$. Returning to the special case $F(n)=0$, we obtain $r=0$ and $t=1$ and thus ballistic transport across the scatterers. Consequently, a chain consisting of identical lattice sites with $F=0$ and $\varepsilon=0$ corresponds to the ideal lead through which electrons are injected in form of Bloch waves from the contacts into the considered disordered chain segment.

In order to obtain the scattering matrix of the total chain of N scatterers from the scattering matrix of the single scatterers, we use an iterative algorithm,[6] which provides for a better numerical stability and efficiency than the previously employed transfer-matrix technique.[4] We assume that the scattering matrix S^{N-1} of a chain of $N-1$ scatterers is known, and simply append the Nth scatterer described by s^N. The essential matrix elements of s^N are again given by Eq. (1) with $i,j=1,2,2N+1,2N+2$.

The matrix elements of the total scattering matrix S^N are obtained by adding all possible paths between each pair of channels, which leads to a geometric series that can be easily summed yielding

$$S^N_{iI}=s^N_{i1}\frac{\chi}{1-z}S^{N-1}_{2I},\quad S^N_{Ii}=S^N_{iI} \tag{6a}$$

$$S^N_{IJ}=S^{N-1}_{IJ}+S^{N-1}_{I2}\chi s^N_{11}\frac{\chi}{1-z}S^{N-1}_{2J}\ , \tag{6b}$$

$$S^N_{ij}=s^N_{ij}+s^N_{i1}\frac{\chi}{1-z}S^{N-1}_{22}\chi s^N_{1j}\ . \tag{6c}$$

Here, $I,J=1,3,4,\ldots,2N$ denote the external channels of S^{N-1} on the left-hand side of Figs. 2(a)–2(c), and $i,j=2,2N+1,2N+2$ label the respective channels of s^N. $z=\chi S^{N-1}_{22}\chi s^N_{11}$ accounts for the multiple reflections between the two scatterers, and $\chi=\exp(iqa)$ describes the phase that the outgoing wave out of channel 2 of S^{N-1} acquires before entering channel 1 of s^N and vice versa. Examples for Eqs. (6a)–(6c) are depicted in Figs. 2(a)–2(c).

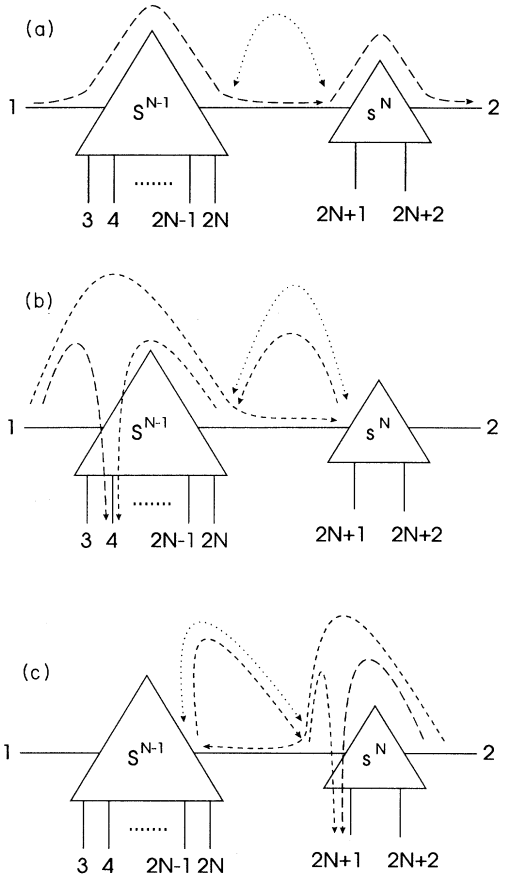

FIG. 2. Scattering processes between external channels of the chain. The long broken lines reflect the direct scattering between the external channels. The short broken lines indicate the indirect way between the external channels. The dotted line denotes the multiple reflections between the scatterers. (a) External channels 1 and 2 as an example of Eq. (6a) with $I=1$ and $i=2$. (b) External channels 1 and 4 as an example of Eq. (6b) with $J=1$ and $I=4$. (c) External channels 2 and $2N+1$ as an example of Eq. (6c) with $j=2$ and $i=2N+1$.

In the following we analyze the transport properties of the chain in terms of the scattering probabilities

$$p_{ij}=|S^N_{ij}|^2 \tag{7}$$

of the chain. These properties depend essentially on the inelastic-scattering strength ε, the disorder strength W, and the chain length N.

III. ELASTIC TRANSMISSION PROBABILITY

An important quantity to describe transport in the coherent regime is the elastic transmission probability $T=p_{21}$, reflecting the direct transmission through the en-

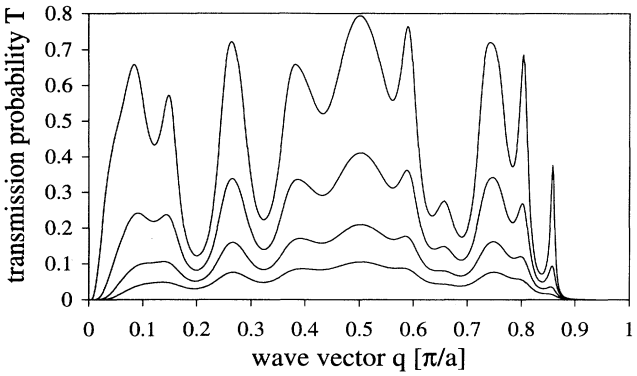

FIG. 3. Elastic transmission probability T vs wave vector (in units of π/a) for a chain of 20 scatterers for $W=1.0$ and the inelastic-scattering strengths $\varepsilon=0.01$, 0.04, 0.07, and 0.1 (from top to bottom). The transmission probability for other wave vectors can be obtained from symmetry considerations yielding $T(q)=T(-q)$.

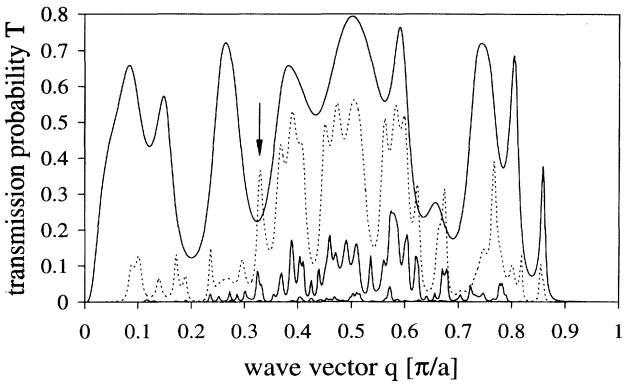

FIG. 4. Elastic transmission probability T for a chain of 20, 50, 100, and 200 scatterers (from top to bottom) for $W=1.0$ and the inelastic scattering strength $\varepsilon=0.01$.

tire chain without diversion into one of the side channels. The dependence of T on the wave vector q is depicted in Fig. 3. In the limit of small ε one can clearly see interference effects due to multiple elastic scattering. Constructive interference leads to peaks in the curve of the transmission probability. The pattern of these peaks depends on the specific realization of the random energies $F(n)$ in a particular sample, and therefore constitutes a fingerprint of the microscopic structure of the sample. With increasing inelastic scattering these oscillations are quickly damped as a consequence of the dephasing of the backscattered waves. Furthermore, one can recognize very small values of T for a range of q values around zero. This corresponds to the occurrence of strongly localized states at the band edges in the Anderson model of localization. In the language of scattered waves (as opposed to the eigenstates) this small transmission shows that the Bloch waves entering the disordered chain (segment) cannot penetrate far into the chain. Comparable states occur as eigenstates in finite chains, localized at the end of the chains. This has led us to label these states surface states in the case of ordered chains. With the exception of very large scattering strength ε, the range of wave vectors for which vanishing elastic transmission can be observed is independent of the inelastic-scattering strength, as can be seen in Fig. 3. This is not surprising because according to Eq. (1) every scattering event leads to diversion of a partial wave from the transport channels into the side channels, but influences only indirectly (namely through the relative amplitudes) the interference between the partial waves remaining in the transport channels.

On the other hand, for longer chains the q window of very small T values increases, because somewhat less localized states fit into the larger sample, or equivalently, waves have to penetrate further in order to pass through the entire sample. This is displayed in Fig. 4.

It is interesting to note that the transmission probability may even increase with increasing chain length. An example is indicated in Fig. 4 by the arrow at $q=0.33$ $[\pi/a]$. This unexpected behavior can also be understood as a consequence of multiple elastic reflections which can enhance the transmission by constructive interference. To display this behavior in more detail, we present the elastic transmission probability versus the chain length in Fig. 5. One can see that the mentioned increase is quite common, but this effect is only important within short segments of the chain; further increasing of the chain length leads to an overall decay of T.

Figure 5 also shows that T decays faster for q values near the band edges than for q values deeper inside the transmission window. This corresponds to the stronger localization of the electronic states near the band edges.

IV. CHARACTERISTIC DECAY LENGTHS

To study the influence of disorder on the elastic transmission probability T, it is useful to define the decay

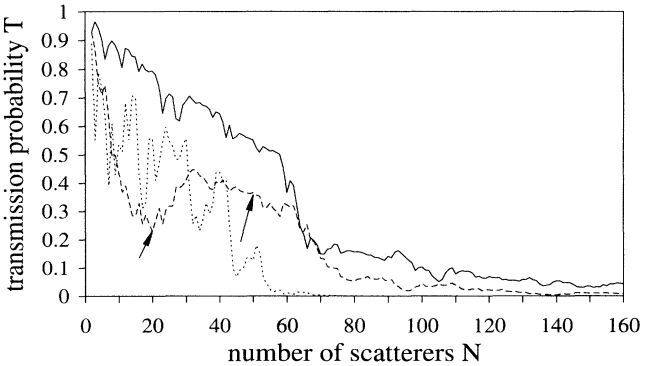

FIG. 5. Elastic transmission probability T vs chain length N for $W=1.0$, $\varepsilon=0.01$, and $q=0.5$ $[\pi/a]$ (full line), $q=0.33$ $[\pi/a]$ (dashed line), and $q=0.1$ $[\pi/a]$ (dotted line). The arrows indicate the values for the chain lengths $N=20$ and 50 for $q=0.33$ $[\pi/a]$ corresponding to Fig. 4.

length $\xi(N)$, which measures the influence of disorder on T:

$$T(\varepsilon,N,W)=T(\varepsilon,N,0)\exp(-N/\xi(N)) . \quad (8)$$

$T(\varepsilon,N,W)$ is the elastic transmission probability of a disordered chain of N scatterers with inelastic-scattering strength ε and disorder strength W; $T(\varepsilon,N,0)$ is the value for the corresponding ordered chain. In the limit of large N, ξ can be interpreted (if it converges) as the localization length of the electron in accordance with the Anderson model ($\varepsilon=0$). Figure 6(a) shows the convergence of $\xi(N)$ for two values of q, namely inside the transmission window at $q=0.75$ $[\pi/a]$ and near the band edge at $q=0.1$ $[\pi/a]$. It can clearly be seen that ξ is much larger inside the transmission window than near the band edges, because the probability for elastic scattering is smaller in the band center.

To study the influence of the inelastic-scattering strength ε on T, we define the decay length $\zeta(N)$ by

$$T(\varepsilon,N,W)=T(0,N,W)\exp(-N/\zeta(N)) . \quad (9)$$

Here $T(0,N,W)$ is the purely elastic ($\varepsilon=0$) transmission probability of a chain of N scatterers with disorder strength W, and $T(\varepsilon,N,W)$ the transmission probability of the same disordered chain with inelastic-scattering strength ε. Again, in the case of convergence for large N, ζ can be interpreted as a mean free path of the electron between two inelastic-scattering processes. Figure 6(b) shows that, for disordered chains up to 1000 scatterers, convergence for ζ cannot be observed for small values of ε. The reason for this behavior are multiple elastic-scattering processes in the transport channel, which locally increase the probability for inelastic scattering within short segments of the chain. We will elucidate on this point in the forthcoming discussion.

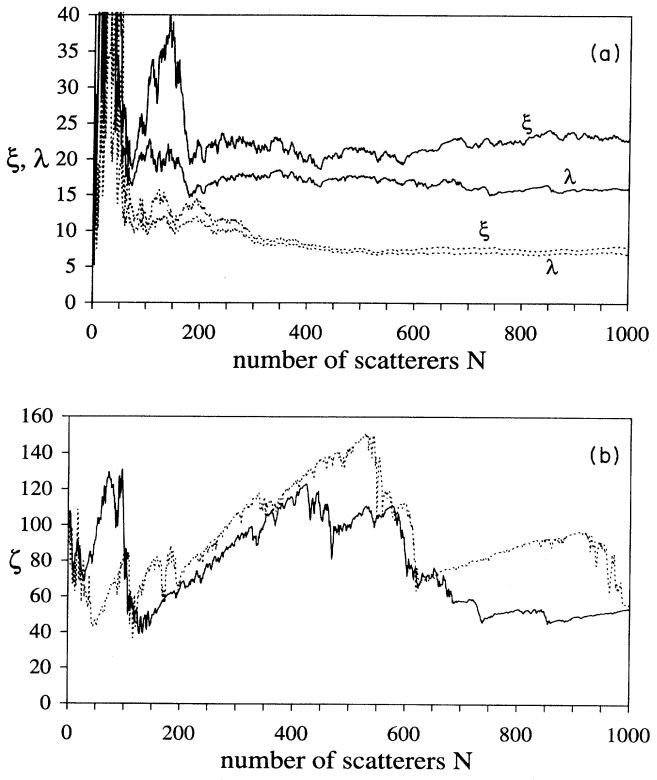

FIG. 6. Decay lengths ξ and λ (a) and ζ (b) vs chain length N for $q=0.75$ $[\pi/a]$ (full lines) and $q=0.1$ $[\pi/a]$ (dotted lines), $W=1.0$ and $\varepsilon=0.01$.

The behavior of the transmission probability in disordered systems may be described by combining these two decay lengths to an effective decay length λ:

$$T(\varepsilon,N,W)=T(0,N,0)\exp(-N/\lambda(N)) . \quad (10)$$

It follows that $\lambda^{-1}(N)=\xi^{-1}(N)+\zeta^{-1}(N)$. Figure 6(a) shows that the overall decay of T is more pronounced if both effects are taken into account. For electrons inside the transmission window, this behavior can clearly be seen. In contrast, the influence of inelastic scattering on electrons near the band edges is very small, because in this case localization is strong anyway. Accordingly the difference between ξ and λ is very small for $q=0.1$ $[\pi/a]$, cf. Fig. 6(a).

V. RESISTANCE

The electrical resistance of a disordered chain is fully determined by its scattering probabilities. For the two-point resistance, the following equation holds:

$$R_{tp}=\frac{h}{2e^2}\frac{1}{p_{21}+\sum_{n=1}^{N}\chi_n(p_{2,2n+1}+p_{2,2n+2})} , \quad (11)$$

where χ_n is given by[4]

$$W_{n0}\chi_n+\sum_{m=1}^{N}W_{nm}(\chi_n-\chi_m)=p_{1,2n+1}+p_{1,2n+2} , \quad (12)$$

with $W_{nm}=p_{2n+1,2m+1}+p_{2n+1,2m+2}+p_{2n+2,2m+1}+p_{2n+2,2m+2}$. The denominator of Eq. (11) can be interpreted as an effective transmission probability, consisting of two parts: the elastic transmission probability p_{21} and the incoherent contribution of electrons, which suffer at least one inelastic-scattering process on their way along the chain. This part, namely the sum in Eq. (11), is called $D(N)$ in the following discussion. Figure 7 shows the dependence of $T(N)$ and $D(N)$ on the chain length. In the limit of short chains and $\varepsilon \ll 1$, D grows as the chain length is increased. By attaching additional scatterers at the end of a chain with high elastic transmission probability, one obtains additional coherent backscattering, and thus the probability for the electron of being inelastically scattered before reaching the end of the chain is increased. This effect vanishes as the length of the chain becomes larger, because the elastic transmission probability becomes very small. Consequently one cannot obtain significant coherent backscattering by attaching additional scatterers. Therefore D decreases as the chain length is increased, because additional scatterers hinder the transport along the chain. In other words, even electrons which have passed through the electron reservoirs do not

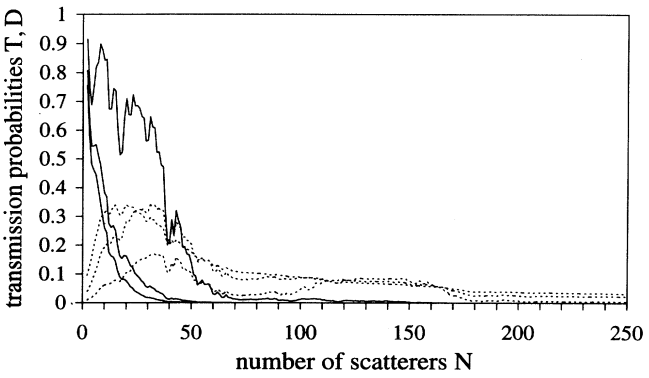

FIG. 7. Transmission probabilities T (full lines) and D (dotted lines) vs chain length N for $W=1.0$ and $q=0.75$ $[\pi/a]$ and $\varepsilon=0.01$, 0.07, and 0.1 (from top to bottom for T, vice versa for D at small N).

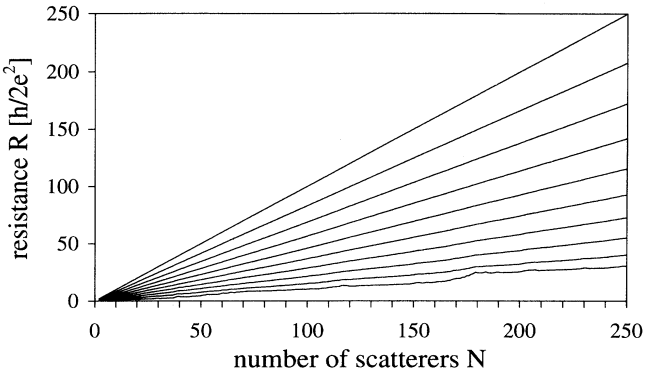

FIG. 9. Resistance R vs chain length N for $W=1.0$, $q=0.75$ $[\pi/a]$, and $\varepsilon=0.1,0.2,\ldots,1.0$ (from bottom to top).

reach the other side of the sample.

In order to obtain the four-probe resistance R, one must subtract the contact resistance R_c from R_{tp}:

$$R=R_{tp}-R_c=R_{tp}-h/2e^2 . \tag{13}$$

Figure 8 shows the four-probe resistance of a chain of 20 scatterers as a function of the wave vector q. One can clearly see, by comparison with Fig. 3, that the characteristic fluctuations of R are fully determined by the elastic transmission probability T. Inelastic processes do not lead to any new structure in the fluctuation pattern. In contrast to $T(q)$, the curves for different ε values in Fig. 8 cross each other at certain q values. This means that an increase of the inelastic-scattering strength can lead to an increase or a decrease of the resistance, depending on the value of q. As a consequence of destructive interference effects, the elastic transmission probability may be very small or even zero for certain q values. This interference behavior is perturbed by waves which have lost their phase memory by the respective inelastic-scattering processes. As a consequence, destructive interference becomes less important with increasing ε, and the resistance R decreases. This behavior can also be investigated by considering Eq. (11). As ε is increased, p_{21} becomes smaller and D becomes larger. Crossings between different ε curves always occur, when the decrease of p_{21} is balanced by the increase of D; the resistance becomes smaller if the increase of D is larger than the decrease of p_{21}. This behavior is most pronounced for q values, at which T is barely affected by changes of ε. Figure 3 shows that this is the case for local minima at low values of T. Contrarily, the resistance increases, if the decrease of p_{21} is larger than the increase of D.

The following figures show the dependence of R on the length of the chain. As can be seen in Fig. 9, no disorder effects show up in the case of fully inelastic transport ($\varepsilon=1$), because transport can only take place via the side channels and is therefore not affected by the disorder in the transport channel. In this limit, we obtain Ohmic behavior. For lower values of ε, the influence of disorder on the resistance can clearly be seen as depicted in Fig. 10. In this figure, the resistance shows two different types of behavior. For chain lengths up to 50 scatterers, R increases with ε, just as in Fig. 9. The decisive term for R is in this case the elastic transmission probability, which

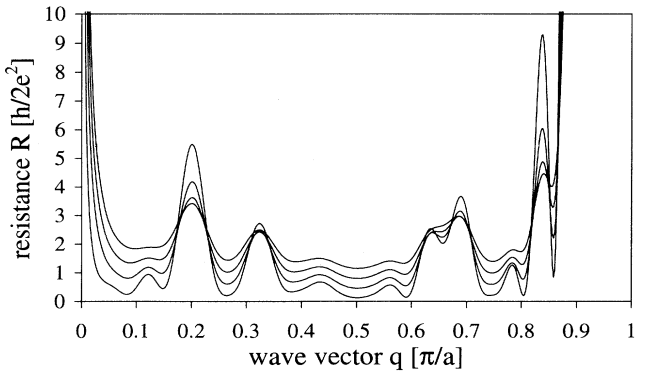

FIG. 8. Resistance R of a chain of 20 scatterers for $W=1.0$ and $\varepsilon=0.01$, 0.04, 0.07, and 0.1 (from bottom to top for small q).

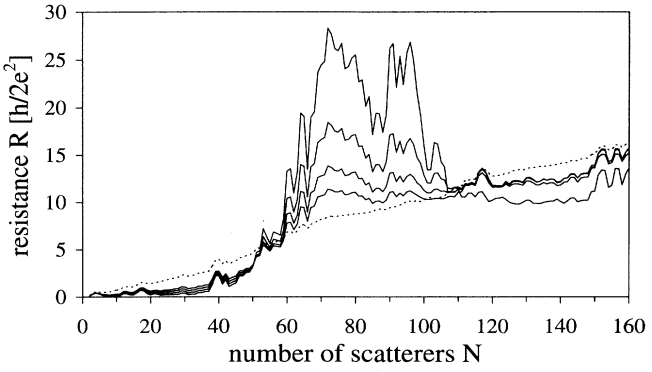

FIG. 10. Resistance R vs chain length N for $W=1.0$, $q=0.25$ $[\pi/a]$, and $\varepsilon=0.01$, 0.02, 0.03, 0.04, and 0.1 (in the center of the figure, around $N=80$ from top to bottom).

is decreasing with increasing ε, leading to an increasing resistance. As the chain becomes sufficiently large, p_{21} becomes relatively small and the behavior of the resistance will be determined mostly by the inelastic transmission probability D. As D increases with ε, the behavior of R in this region is exactly inverted, at least for small ε values. With the further increase of ε, the system again tends to Ohmic behavior. For chain lengths between 110 and 160 scatterers, the behavior of the resistance cannot be described distinctly. It is very interesting to note that the decay length ζ, which describes the influence of inelastic scattering on T, decays very strongly in the region between the 100th and 110th scatterers (not shown here). This means that inelastic coupling affects the behavior of the electrons very strongly in this region, as they can travel only short distances between two inelastic collisions. This behavior can also be seen in Fig. 7, where D begins to grow at the 100th scatterer for small values of ε. In a region of small T this leads to a decrease of R, because the electron can only pass the chain by using side channels. The reasons for this behavior are multiple reflections in the transport channel, which locally increase inelastic scattering, as mentioned above in the discussion of Fig. 6(b). Therefore it is understandable that this effect vanishes with increasing ε, or alternatively with decreasing disorder strength W, because multiple reflections become less important in both cases.

Disorder effects are suppressed as q approaches the center of the transmission window. For $q=0.5\ [\pi/a]$, $T(q)$ has a maximum. Consequently, multiple elastic reflections are not that likely anymore, and the influence of disorder on the transport properties of the system shrinks. This corresponds to the well-known fact that electron states near the band center are less localized.

VI. CONCLUDING REMARKS

In this paper, we have studied the essential transport properties of a linear site-disordered chain by means of a scattering matrix technique. We wish to point out that all results in this paper refer to the same disordered microstructure. Different configurations show different fluctuation patterns, and configurational averages lead to vanishing fluctuations. The calculation of the coherent reflection and transmission coefficients are based on a nearest-neighbor tight-binding model. Inelastic processes are introduced by means of a parameter ε, which controls the scattering probability into the electron reservoirs. In the limit of coherent transport, we obtain strong fluctuations as a result of multiple reflections between the single scatterers. As we increase the inelastic-scattering strength ε, these oscillations are suppressed; in the case of $\varepsilon=1$, all oscillations vanish and Ohmic behavior shows up. Thus we are able to describe the extreme cases of coherent and incoherent transport as well as the intermediate behavior. In the latter case we have shown that the transport properties of the system depend strongly on the energy of the electron and the interplay between interference and dephasing effects.

We conclude that our calculations reproduce well-known results, but in contrast to previous works which use parametrized scattering coefficients our calculations are based on a well-defined tight-binding Hamiltonian for elastic scattering. Currently, this Hamiltonian is being extended to include inelastic scattering as well.

*Present address: Institut für Physik, Technische Universität Chemnitz-Zwickau, D-09107 Chemnitz, Federal Republic of Germany.

[1]For an overview see, e.g., *Quantum Coherence in Mesoscopic Systems*, edited by B. Kramer (Plenum, New York, 1991).

[2]R. Landauer, IBM J. Res. Dev. **1**, 223 (1957); Philos. Mag. **21**, 863 (1970); Z. Phys. B **68**, 217 (1987); J. Phys. Condens. Matter **1**, 8099 (1989).

[3]M. Büttiker, Phys. Rev. B **33**, 3020 (1986).

[4]K. Maschke and M. Schreiber, Phys. Rev. B **44**, 3835 (1991).

[5]M. Schreiber and K. Maschke, Z. Phys. B **85**, 123 (1991).

[6]M. Schreiber and K. Maschke, Philos. Mag. **65**, 639 (1992).

[7]K. Maschke and M. Schreiber, Phys. Rev. B **49**, 2295 (1994).

[8]J. L. D'Amato and H. M. Pastawski, Phys. Rev. B **41**, 7411 (1990).

[9]S. Datta, J. Phys. Condens. Matter **2**, 8023 (1990).

[10]M. Cahay and S. Bandyopadhyay, Phys. Rev. B **42**, 5100 (1990).

[11]S. Gangopadhyay and A. K. Sen, J. Phys. Condens. Matter **4**, 9939 (1992).

[12]P. A. Schulz, D. S. Galvão, and M. J. Caldas, Phys. Rev. B **44**, 6073 (1991).

[13]A. K. Sen and S. Gangopadhyay, Physica A **186**, 270 (1992).

[14]P. W. Anderson, Phys. Rev. **109**, 1492 (1958).

[15]R. P. Feynman, R. B. Leighton, and M. Sands, *Lectures on Physics III (Commemorative Issue)* (Addison-Wesley, Reading, MA, 1989), p. 13-11.

[16]F. Gagel and K. Maschke, Phys. Rev. B **49**, 17 170 (1994).

[17]G. Burmeister, K. Maschke, and M. Schreiber, Phys. Rev. B **47**, 7095 (1993).